Nanoscale Elastic-Property Mapping with Contact-Resonance-Frequency AFM*

D. C. Hurley, A. B. Kos, and P. Rice
National Institute of Standards & Technology
Boulder, CO 80302-3328, U.S.A.

ABSTRACT

We describe a dynamic atomic force microscopy (AFM) method to map the nanoscale elastic properties of surfaces, thin films, and nanostructures. Our approach is based on atomic force acoustic microscopy (AFAM) techniques previously used for quantitative measurements of elastic properties at a fixed sample position. AFAM measurements determine the resonant frequencies of an AFM cantilever in contact mode to calculate the tip-sample contact stiffness k^*. Local values for elastic properties such as the indentation modulus M can be determined from k^* with the appropriate contact-mechanics models. To enable imaging at practical rates, we have developed a frequency-tracking circuit based on digital signal processor architecture to rapidly locate the contact-resonance frequencies at each image position. We present contact-resonance frequency images obtained using both flexural and torsional cantilever images as well as the corresponding vertical contact-stiffness (k^*) image calculated from flexural frequency images. Methods to obtain elastic-modulus images of M from vertical contact-stiffness images are also discussed.

INTRODUCTION

As critical dimensions shrink below 1 μm, new tools are required to investigate material properties on commensurate scales. In particular, nanomechanical information—knowledge on nanometer length scales of mechanical properties such as elastic modulus, strength, adhesion, and friction—is needed in many emerging applications. The need is driven by the increasing integration of multiple materials on micrometer and nanometer scales. The complexity of such systems increases the demand for accurate property values for predictive modeling. Furthermore, because localized variations in properties are often the cause of failure, it is increasingly important to assess not just the “average” properties from a single sample position, but to visualize spatial variations in properties.

One approach to meet this objective combines nanoindentation techniques with force modulation and scanning [1]. This promising method is limited in lateral spatial resolution by the radius (a few hundred nanometers) of the Berkovich diamond indenter used. Therefore, methods that exploit the increased spatial resolution of atmomic force microscopy (AFM) are also being developed. Those methods that promise quantitative image information are typically dynamic approaches in which the AFM cantilever is vibrated at or near the frequencies of its resonant modes. Two of these approaches are contact methods called ultrasonic AFM [2,3] and atomic force acoustic microscopy (AFAM) [4,5]. In this paper, we describe our progress towards quantitative imaging of nanoscale elastic properties using AFAM. Using new signal acqusition and processing techniques, we have modified methods previously demonstrated for quantitative fixed-point measurements [6,7] to achieve rapid imaging of contact-resonance frequencies. From such images, modulus maps may ultimately be determined.

EXPERIMENTAL METHODS

AFAM Techniques

The experimental methods and theoretical basis for determining elastic properties using AFAM have been described in detail elsewhere [6, 7]. In summary, vibrations in the range of 10 kHz to 3 MHz are excited in the sample of interest by an ultrasonic piezoelectric transducer mounted beneath it. When the tip of the AFM cantilever is in contact with the sample, the vibrations are coupled into the cantilever. Vibrations at the appropriate frequencies excite resonant modes of the cantilever beam. The amplitude of cantilever vibration at the transducer excitation frequency, and hence the frequencies of the resonant modes (the "contact-resonance frequencies"), are detected from the AFM photodiode signal using a lock-in amplfier. From the contact-resonance frequencies of the first two flexural (bending) modes, the value of the indentation modulus M can be determined [7,8]. For an isotropic material, $M = E/(1-\nu^2)$, where E is Young's modulus and ν is Poisson's ratio. Torsional cantilever modes may also be measured in a similar fashion. For isotropic materials, the elastic quantity that can be determined from torsional-mode frequencies is $G = E/2(1+\nu)$ [9]. Thus, by combined measurements of M and G, it is theoretically possible to simultaneously determine E and ν independently. Although this fact has been mentioned in the literature [9], to our knowledge it has not yet been experimentally demonstrated.

Resonance-Frequency Tracking Electronics

Directly applying the AFAM methods described above for elastic-property imaging is not practical, because lock-in techniques are typically much too slow. One author estimated that several days would be needed to acquire a single image in this way [2]. This problem has previously been addressed [2,3,5]. Our approach towards overcoming this difficulty involves new signal acquisition and processing methods based on a 32-bit floating-point digital signal processor (DSP). A block diagram of the circuit is shown in Fig. 1. Briefly, the circuit applies an adjustable-amplitude, swept-frequency sinusoidal voltage to the piezoelectric transducer beneath the sample. A wideband, root-mean-square-to-DC (RMS-to-DC) converter fed by a low-noise operational amplifier with a noninverting gain of 100 is used to detect the magnitude of the photodiode signal and deliver it to an analog-to-digital converter. The RMS-to-DC converter has a flat bandpass response from approximately 1 kHz to 3.2 MHz. From the RMS voltage response as the frequency is swept, the circuit constructs a complete resonance curve and finds its peak. This information is sent to a digital feedback control loop that adjusts a voltage-controlled oscillator (VCO) to tune the center frequency of vibration, keeping the center of the sweep window centered on the cantilever resonance. The control voltage is also sent to the AFM's auxiliary image input port. Thus each pixel in the acquired image contains a value proportional to the peak (resonant) frequency at that position. A frequency range can be specified in order to exclude all but the cantilever mode of interest.

Some of the most important features of the DSP circuit include an enhanced direct memory access (DMA) controller that enables data acquisition independent of the DSP core, a multichannel buffered serial port to communicate with the analog-to-digital (A/D) and digital-to-analog (D/A) converters, and a multi-unit processor core capable of 600 million floating

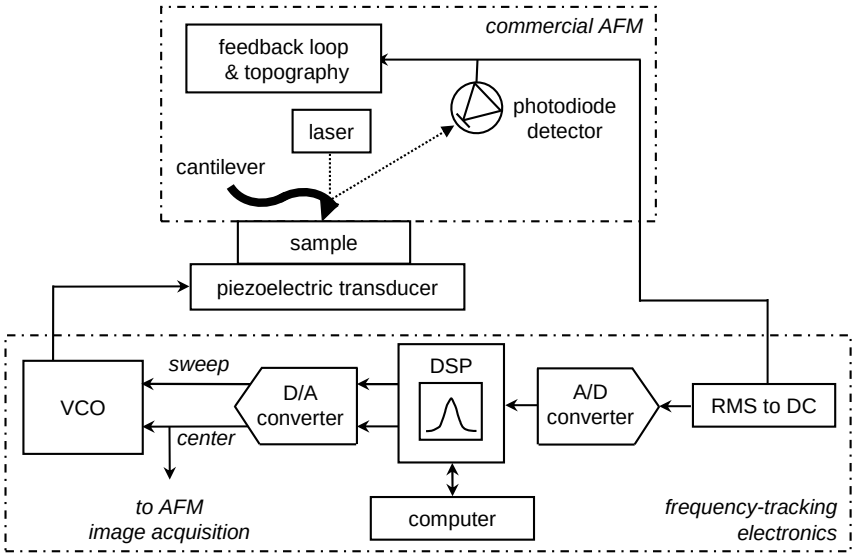

Figure 1. Block diagram of the resonance-frequency tracking circuit used in this work.

point operations per second. The 20-bit delta-sigma A/D and D/A converters are located on a stereo audio daughtercard mated to the DSP board and operate at 48 kilosamples per second. At 48 kilosamples per second and 128 samples per spectrum, the system is capable of acquiring the full cantilever resonance spectrum every 2.7 ms (375 Hz repetition rate). In its current form, the circuit realizes approximately 17-18 bits of resolution, corresponding to an intrinsic frequency resolution of $\sim$12 Hz over a full-range span of 3 KHz to 3 MHz.

RESULTS AND DISCUSSION

The frequency-tracking electronics were used to acquire contact-resonance frequency images for a variety of samples. The sample used for the images shown here contained a stack of two thin films deposited on a silicon wafer with microfabrication techniques. The top film was a niobium (Nb) "wire" $\sim$200 nm thick and 4 μm wide. The Nb film was sputtered on top of a blanket film of silica (SiO_2) $\sim$350 nm thick created by plasma-enhanced chemical vapor deposition.

Quantitative fixed-point AFAM experiments [6] were performed to independently determine the elastic properties of the constituent films. For these measurements, a reference sample of fused silica was used. We assumed a value of the indentation modulus for the reference material $M_{\mathrm{ref}} = 74.9$ GPa based on ultrasonic pulse-echo measurements of similar fused-silica samples. A total of 28 measurements on the SiO_2 film yielded an average value of $M_{\mathrm{SiO2}} = 75.1 \pm 10.0$ GPa, while 22 measurements on the Nb film gave $M_{\mathrm{Nb}} = 112.7 \pm 15.0$ GPa. The uncertainties represent the standard deviation in the individual measurements. The values for M were obtained assuming Hertzian (spherical) contact between the tip and sample. These results are in good agreement with the range of literature values for bulk fused silica ($M_{\mathrm{SiO2}} \approx$ 72-77 GPa) and bulk Nb ($M_{\mathrm{Nb}} \approx$ 116-133 GPa).

Contact-resonance frequency images for the Nb/SiO_2 sample are shown in Figs. 2(a) and (b) for the first (f_1) and second (f_2) flexural modes, respectively. To acquire these images, we used a

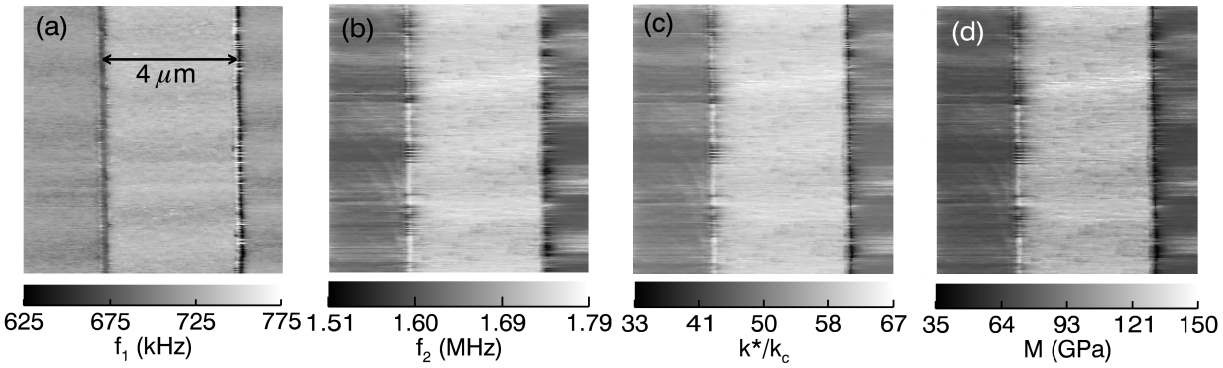

Figure 2. Contact-resonance frequency images of (a) the first flexural mode f_1 and (b) the second flexural mode f_2 for a Nb/SiO_2 sample. (c) Corresponding image for the normalized vertical contact stiffness k^*/k_c calculated from the frequency images in (a) and (b). (d) Corresponding image of the indentation modulus M calculated from (c), assuming Hertzian contact mechanics.

silicon cantilever approximately 225 μm long, 34 μm wide, and 7.1 μm thick. The nominal value of the cantilever spring constant provided by the vendor was $k_c = 47$ N/m, while the measured free-space resonant frequencies of the first two flexural modes were respectively 167.55 and 1044.0 kHz. The central Nb stripe stands out clearly in contrast to the left and right regions of SiO_2 film. The narrow, bright and dark vertical lines in Figs. 2(a) and (b) indicate relatively large frequency changes that occur at the interfaces between the SiO_2 and Nb films. Presumably, these are topography-induced frequency shifts caused by transient changes in the contact area as the tip moves from one material to another. The frequency information in these narrow regions are not deemed reliable. However, the values of f_1 and f_2 for the individual materials are reasonably uniform and repeatable from line to line. The images also show that both f_1 and f_2 are greater for the Nb film, suggesting that the contact stiffness is greater here. This hypothesis is verified in Fig. 2(c), which contains a map of the normalized contact stiffness k^*/k_c obtained using Figs. 2(a) and (b). Figure 2(c) was calculated using standard AFAM methods that assume a variable tip position to determine k^*/k_c from the contact-resonance frequencies [7].

Although contact-stiffness images are useful for visualizing relative variations in properties, our ultimate objective is a direct map of the sample's elastic properties. AFAM experiments typically use measurements of a reference material in tandem with measurements of the unknown material to determine M from the measured values of k^*/k_c [8]. This approach avoids direct determination of the contact radius, which is difficult in practice and complicated by wear of the silicon tip. We found experimentally that the tip-sample contact for a moving tip differed from that of a static contact. Therefore, instead of comparing the values of k^*/k_c in Fig. 2(c) to those from point measurements of a reference sample, we applied a "self-calibrating" approach. We assumed that the mean value of k^*/k_c for the SiO_2 region corresponded to the previously measured value of $M_{SiO2} = 75.1$ GPa. With this assumption and using the Hertzian contact model, values of M for the entire image were calculated. The corresponding image, shown in Fig. 2(d), indicates that the values obtained are physically reasonable. The mean value of the entire region of SiO_2 film is $M_{SiO2} = 75.5 \pm 7.1$ GPa. The mean value of the Nb film region is $M_{Nb} = 118.5 \pm 7.1$ GPa. This is in good agreement with both the fixed-point value of 112.7 $\pm$ 15.0 GPa obtained above and with literature values of 116 to 133 GPa. Both of these results were

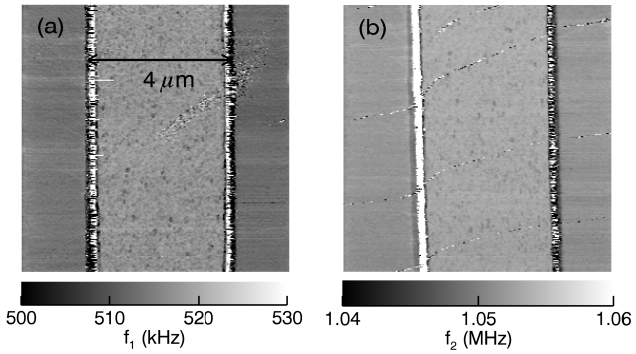

Figure 3. Torsional contact-resonance frequency images of the Nb/SiO_2 sample: (a) the first mode f_1, and (b) the second mode f_2. The diagonal streaks are probably the result of sample contamination.

calculated from image regions containing more than 2×10^4 pixels. Furthermore, the relatively small standard deviation of the results indicates that the tip-sample contact is relatively consistent and repeatable for a given material. Using this fact, it may be possible to obtain quantitative AFAM results more quickly and precisely by acquiring frequency images over a small region of the sample.

We also obtained contact-resonance frequency images for torsional (twisting) modes of the AFM cantilever. To perform these experiments, we modified our AFM to allow detection of the horizontal (left minus right) signal of the quadrant photodiode in the kilohertz to megahertz frequency range. For the torsional experiments we used a silicon cantilever approximately 448 μm long, 51 μm wide, and 3.5 μm thick with $k_c = 0.98$ N/m (vendor value). The cantilever's torsional modes were excited by an ultrasonic transducer that generated in-plane (shear) vibrations. The measured free-space frequencies of the first two torsional modes of this cantilever were 340.1 and 1022.3 kHz, respectively. Torsional contact-resonance frequency images obtained with this cantilever for the Nb/SiO_2 sample are shown in Fig. 3. Like the flexural-frequency images in Fig. 2, the torsional images show large topography-induced frequency shifts at the interfaces between the two different materials. In contrast to the flexural modes, however, the first torsional mode appears more sensitive than the second, exhibiting greater changes in frequency from material to material. The frequency changes for the second mode are quite small between the SiO_2 and Nb regions. Nonetheless, the frequencies of both modes are higher for the Nb region than for the SiO_2 regions. This suggests that the lateral contact stiffness (and thus, by inference, G) is higher for the Nb film. This behavior is qualitatively consistent with literature values of E and ν for bulk Nb. We are working to develop an analysis procedure for converting the torsional frequency images into quantitative lateral-stiffness images.

With our specific circuit components, the frequency-tracking electronics perform a frequency sweep (*i.e.*, acquire a spectrum) at a repetition rate of 375 Hz, or approximately every 2.7 ms. The scanning speed and number of points per image line must be adjusted so that several sweeps are performed at each image position. The scan size and contrast in elastic properties (*i.e.*, the relative frequency shift) also affect the acquisition rate. We found that for scans a few to several micrometers in size, it was usually sufficient to operate at a scan rate of 0.2 Hz (5 s/line) when acquiring images 256 pixels wide. At a scan rate of 0.2 Hz, a 256×256 image requires ∼22

minutes. Thus, it takes less than one hour to acquire frequency images for two resonant modes. This period can be reduced by upgrading the electronics components with newer (faster) models. The corresponding contact-stiffness (k^*/k_c) and modulus (M) images are calculated separately from custom subroutines written for commercial image-analysis software. These calculations (which have not been optimized for speed) take less than about 10 minutes.

SUMMARY AND CONCLUSIONS

We have described our progress towards the goal of quantitative elastic modulus imaging using AFAM methods. Frequency-tracking electronics have been developed to rapidly image the contact-resonance frequency in a given region of the sample surface. To illustrate the flexibility of our methods, images corresponding to the first two flexural and torsional modes were presented for a Nb/SiO_2 sample. From the flexural frequency images, a map of the normalized tip-sample contact stiffness k^*/k_c was calculated. A quantitative image of the indentation modulus M was obtained from the k^*/k_c image using independent knowledge of the constituent elastic properties and assuming Hertzian contact mechanics. Values of M obtained for both the SiO_2 and Nb films were physically realistic and in good agreement with previous fixed-position measurements, increasing our confidence in the basic approach. Although these results are promising, achieving the goal of quantitative modulus mapping requires further effort to understand and control such issues as surface topography, tip wear, and the actual tip-sample contact behavior.

ACKNOWLEDGEMENTS

The Nb/SiO_2 sample was provided by G. C. Hilton (NIST). We thank C. Su (Veeco-DI) and M. Kopycinska-Müller (NIST) for valuable discussions.

REFERENCES

1. S. A. Syed Asif, K. J. Wahl, R. J. Colton, and O. L. Warren, *J. Appl. Phys.* **90**, 1192 (2001).
2. K. Yamanaka, Y. Maruyama, T. Tsuji, and K. Nakamoto, *Appl. Phys. Lett.* **78**, 1939 (2001).
3. K. Kobayashi, H. Yamada, and K. Matsushige, *Surf. Interface Anal.* **33**, 89 (2002).
4. U. Rabe, M. Kopycinska, S. Hirsekorn, J. Muñoz Saldaña, G. A. Schneider, and W. Arnold, *J. Phys. D: Appl. Phys.* **35**, 2621 (2002).
5. E. Efimov and S. A. Saunin, in *Proceedings of the Scanning Probe Microscopy Conference* (Nizhny Novgorod, 1-6 March 2002), pp. 79-81; http://www.nanoworld.org/english/SPM2002/contents.htm (accessed November 2004).
6. D. C. Hurley, K. Shen, N. M. Jennett, and J. A. Turner, *J. Appl. Phys.* **94**, 2347 (2003).
7. U. Rabe, S. Amelio, E. Kester, V. Scherer, S. Hirsekorn, and W. Arnold, *Ultrasonics* **38**, 430 (2000).
8. U. Rabe, S. Amelio, M. Kopycinska, S. Hirsekorn, M. Kempf, M. Göken, and W. Arnold, *Surf. Interf. Anal.* **33**, 65 (2002).
9. K. Yamanaka and S. Nakano, *Appl. Phys. A* **66**, S313 (1998).